Chemical Structure and Compatibility of Polyamide–Chitin and Chitosan Blends

VIRGILIO GONZÁLEZ, CARLOS GUERRERO, UBALDO ORTIZ

Universidad Autónoma de Nuevo León, FIME, Pedro de Alba S/N, Cd. Universitaria, San Nicolás, N.L., 66450 México

Received 16 September 1999; accepted 3 March 2000

ABSTRACT: This work presents a comparative study of the compatibilization of four binary blends with slight differences in their chemical structures. The natural polymers chitin (QA) and chitosan (QN) are blended with polyamide 6 (PA6) and polyamide 66 (PA66). The results, obtained using differential scanning calorimetry, infrared spectroscopy, and light and scanning electron microscopy, gave the following compatibilization sequence: PA6/QN ≈ PA66/QN > PA6/QA > PA66/QA. This behavior could be related to the ability of QN to form hydrogen bonds and also to the capability of the packing of PA66. © 2000 John Wiley & Sons, Inc. J Appl Polym Sci 78: 850–857, 2000

Key words: chitin; chitosan; polyamide; blends; compatibilization

INTRODUCTION

The exoskeleton of crabs, shrimps, and lobsters are very important waste materials in the fishing industry because they are a source of raw material for chitin and chitosan production.[1,2] The technological importance of these natural polymers consists of their ability to promote chemical interactions with proteins. In our case, it is very attractive to analyze the effect of the slight structural differences between poly-*N*-acetyl-D-glucosamine) (QA) and its derivative deacetylated QA (QN) (Fig. 1) regarding the chemical interactions with other polymers with structures similar to those of protein, such as polyamides. This study could be more attractive if we chose two polyamides with also slight structural differences, like polyamide 6 (PA6) and polyamide 66 (PA66) (Fig. 2).

In accordance with the theory of Flory–Huggins,[3,4] the miscibility and compatibility of two polymers depend essentially on their ability to form specific interactions between them, which contributes to diminish or make negative the mixing enthalpy (ΔH_m). For example, the formation of hydrogen bonds between two different macromolecules competes with the formation of hydrogen bonds between molecules of the same polymer. The latter does not contribute to the ΔH_m. Then, it is expected that the intensity of the hydrogen bonding and the steric effect would be the determinants for the compatibility and miscibility of the two polymers.

In analyzing the QA structure, it can be noticed that this macromolecule could form different types of hydrogen bonds with another QA macromolecule: (a) between two hydroxyl groups (HO—OH), (b) between the hydrogen of the amide group and the oxygen of the hydroxyl group (NH—OH), and the stronger bond (c) between the hydrogen of heteroatoms and the carbonyl group of the amide (C═O—HO and C═O—HN). Moreover, the acetyl group of QA could represent a steric impediment on the formation of hydrogen bonds involving either the nearest hydroxyl group or the hydrogen of the amine. Chances of interactions between carbonyl groups of two QN molecules are

Correspondence to: C. Guerrero.

Contract grant sponsor: National Science and Technology Council (CONACyT).

Journal of Applied Polymer Science, Vol. 78, 850–857 (2000)

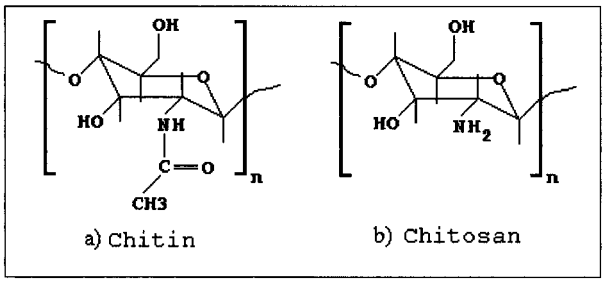

Figure 1 Chemical structure of (a) chitin and (b) chitosan.

quite low, because the QN formation implies the deacetylation of QA. If it is blended with another polymer, then QN could be more effective than is QA on the formation of hydrogen bonds.

The only structural difference between PA6 and PA66 is the number of methylene groups between amide groups. PA6 has only five methylene groups, while PA66 has four methylene, one amide, and then another six methylene groups. This difference promotes better molecular packing of PA66, increasing the possibility of forming hydrogen bonds between PA66 molecules. Then, when PA66 is blended with different polymers, it could be difficult for the functional groups of the other polymers to break the PA66 molecular hydrogen bonds and have interaction with them.

As stated previously, miscibility, and compatibility, between two polymers depends on its specific interactions, such as hydrogen bonds. This kind of interaction could be detected using spectroscopic techniques,[5–7] displaying displacements or widening of the infrared spectra of the functional groups involved. The chemical potentials of blended materials also change, decreasing the enthalpy and melting temperature and modifying the vitreous transition temperature of polymers. These phenomena could be analyzed using differential scanning calorimetry. If blended polymers are immiscible, different phases would be easily detected either by optical or electronic microscopy. The aim of this work was to present the results of a structural (FTIR), thermodynamic (DSC), and morphological (SEM and optical microscopy) analysis of binary blends made of PA6/QN, PA6/QA, PA66/QN, and PA66/QA.

EXPERIMENTAL

Raw Materials

The PA6 for monofilaments was from Celanese Mexicana, while the PA66 injection-molding frame was from BASF. QA and QN were obtained from crab shells, the latter with 72% deacetylation. Both biopolymers were from Sigma Co. All the resins were obtained by Mexican Suppliers (Mexico City).

The molecular weight distribution of polyamides was obtained through the size exclusion chromatography technique using a Waters GPC-150C chromatograph.[8] The thermal transitions were determined with a DSC 1090 from DuPont at 10°C/min in a N_2 atmosphere at 100 mL/min.

The deacetylation degree of chitin and chitosan was obtained through infrared spectroscopy, following the method proposed by Moore[9] and Domszy[10]; the equipment used was an FTIR Nicolet 710. The molecular weight was measured using capillary viscometry, dissolving the materials in solvents for which the Mark–Houwink constants are reported. The solvents were a buffer of CH_3COOH 0.2*M*/CH_3COONa 0.1*M* for QN[11] and formic acid for QA.[12] QA was dissolved following the methods previously reported.[13,14] The results of this characterization are shown in Tables I and II. Films of QA and QN were also analyzed with a Siemens D-5000 X-ray diffractometer.

Blends

Blends were prepared by solvent-evaporation at 30°C from 1 wt % formic acid solutions. Several

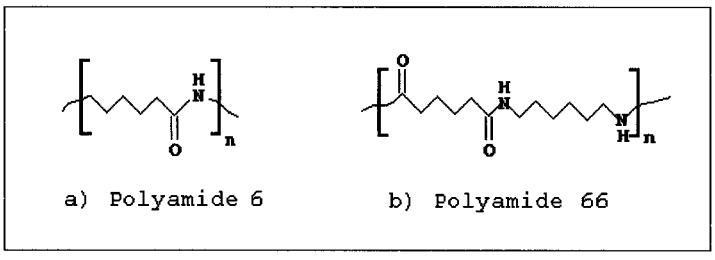

Figure 2 Chemical structure of (a) PA6 and (b) PA66.

Table I Some Properties of the Polyamides Used in This Work

Sample	M_n	M_w	MWD	T_g (°C)	T_m (°C)	ΔH_m (cal/g)	$(1 - \lambda)$ (%)
PA6	46,800	80,600	1.72	45.3	209.3	14.3	31[a]
PA66	38,500	91,000	2.37	51.7	255.2	11.0	18[a]

[a] The degree of crystallization $(1 - \lambda)$ was estimated using the equilibrium melting enthalpies reported by Magill et al.[15] and Inoue.[16]

PA6/QA, PA6/QN, PA66/QA, and PA66/QN concentration samples ranging from 100/0 to 0/100 were prepared. The obtained films were washed several times with distillated water and then dried in a lyophilizer for 4 h. The dried samples were kept in a P_2O_5 dessicator.

The thermal characterization was made as previously mentioned at temperatures ranging from −150 to 300°C. Prior to the FTIR measurements, the samples were heat-treated at 160°C for 3 min; then, the spectra were obtained with at least 65 scans per sample and a 2-cm^{-1} resolution. The morphology of the samples was observed using both a cross-polarized Olympus optical microscope and a Phillips XL-30 scanning electron microscope with an EDX X-ray spectrometer. For SEM analysis, the samples were gold-sputtered.

RESULTS AND DISCUSSION

The polymer solutions and their blends were homogeneous and transparent, passing from colorless to slightly yellowish as the QA or QN content increased. The obtained films were tough, flexible, and translucid, but they became softer when immersed in water. The X-ray diffraction pattern of QA and QN films did not show any peak, which indicates the absence of crystallinity.

As previously stated, it is expected that QN has a greater capability than has QA for the formation of hydrogen bonds when blended with other materials; consequently, chitosan will be more hygroscopic. The thermogravimetric curve (Fig. 3) for QA and QN shows that the latter has twice as much water as has QA. DSC analysis of samples heated at different temperatures[18,19] (Fig. 4) also shows that the water content is always greater in QN. These results support the structural analysis described above.

Table II Molecular Weight (M_v) Intrinsic Viscosity ([η]) and Deacetylation Degree (GD) of Biopolymers

Sample	GD[a] (%)	[η] (g/dL)	M_v (g/mol)
QA[b]	49	14.36	840,100
QN[c]	79	4.04	502,600

[a] According to Moore[9] and Domszy.[10]
[b] Mark–Houwink constants reported by Muzzarelli.[12]
[c] Mark–Houwink constants reported by Rathke and Hudson.[17]

Thermal Analysis

Figure 5 presents the thermal transitions for the four analyzed blends. There are two endotherms; the first one corresponds to a loss of absorbed water, while the second endotherm is related to the polyamide fusion.[18,19] As the polyamide content increases, the intensity of the dehydration endotherm decreases. With PA66/QN blends, the melting temperature occurs very close to the QN degradation temperature; therefore, a meticulous analysis of the enthalpy of fusion (ΔH_m) must be performed.

The dehydration enthalpy, ΔH_{dh}, of the blends is presented in Figure 6. For the PA6/QN samples, the humidity of the specimens increases linearly with the QN content in all the composition

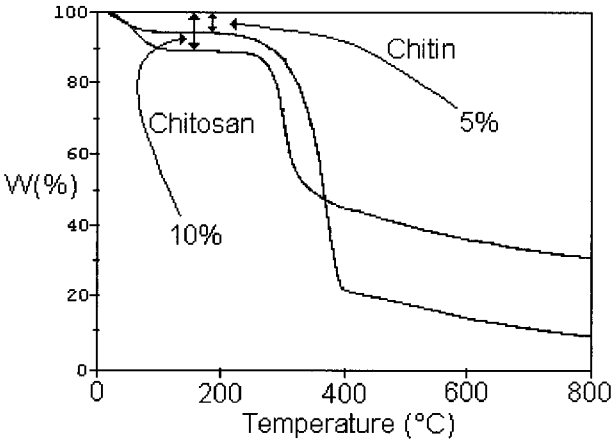

Figure 3 TGA thermograms for chitin and chitosan.

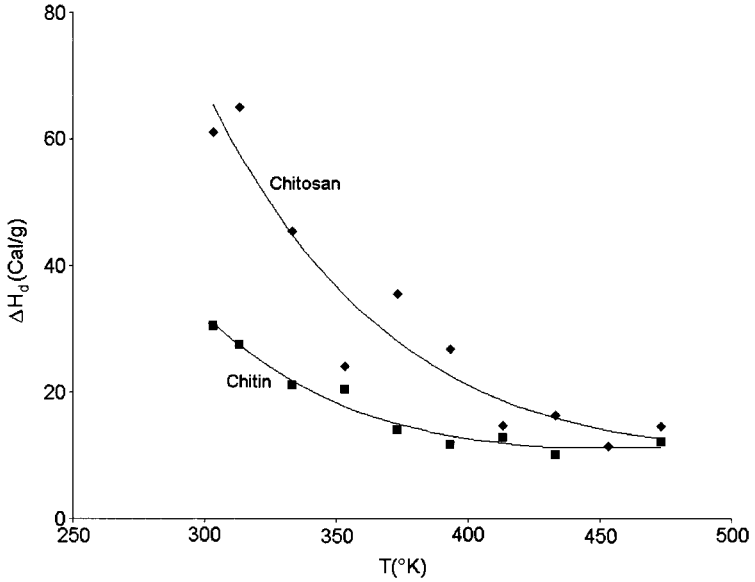

Figure 4 Effect of heat treatment on the dehydration enthalpy of chitin and chitosan.

ranges and it could be possible to estimate the ΔH_{dh} as a function of the biopolymer content. For all the other blends, the slope of the curve changes at about 50% of the biopolymer content, which is associated with a probable phase inversion.

The melting temperature of the blends remains independent of the QA and QN composition. In fact, the second thermal transition of the PA66 blends was at 257.8 ± 1.3°C and 219.5 ± 0.6°C for the PA6 blends. The measured heat of fusion was normalized with respect to the weight fraction of the polyamide in the blend and then plotted against the biopolymer composition (Fig. 7). All the blends show a decrement on the heat of fusion except the PA66/QA blend. Similar behavior was previously reported by Ratto and coworkers,[20,21] but for QN/PA4 blends.

The decrement on ΔH_mcould be interpreted as a variation of the polyamide chemical potential on the blend, modifying its crystallization behavior or, with the formation of an amorphous polyamide/biopolymer phase, decreasing the percentage of crystallized polyamide with respect to the overall mass of the sample. The latter assumption is well supported by the knowledge related to the melting point of polyamides, which is practically not affected by the biopolymer content.

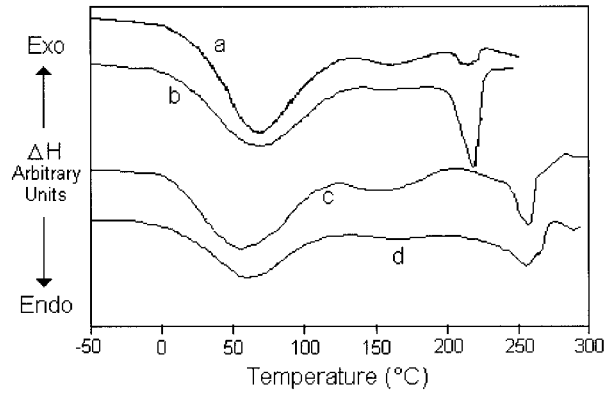

Figure 5 DSC blend thermograms: (a) PA6/QN 50/50; (b) PA6/QA 70/30; (c) PA66/QA 60/40; (d) PA66/QN 70/30.

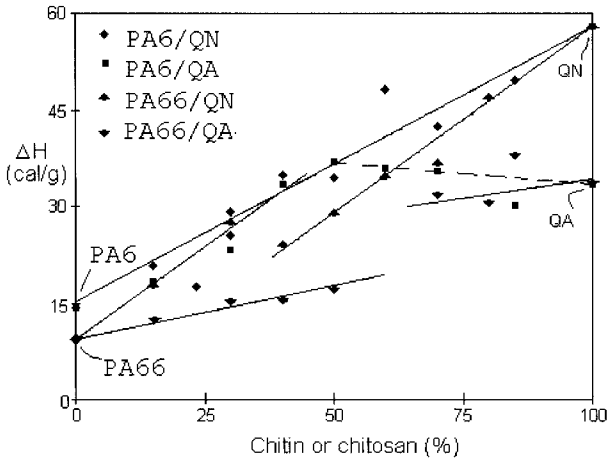

Figure 6 Dehydration enthalpy versus QA and QN content for different blends.

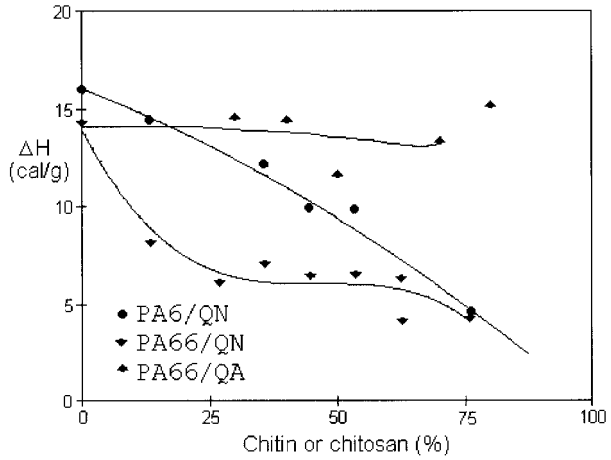

Figure 7 Normalized melting enthalpy versus QA and QN content for different blends.

Infrared Spectroscopy

Figure 8 shows FTIR spectra for different PA6/QN blends. Attention must be paid to the displacement of the carbonyl band of the amide group of QN, located at 1655 cm^{-1}, up to 29 cm^{-1} toward smaller wavenumbers (smaller energy). A similar behavior is observed in PA66/QN blends (Fig. 9). This behavior could be attributed to the fact that hydrogen bonds formed between macromolecules of different polymers are stronger than are those existing originally between the QN molecules. On the other hand, the FTIR measurements on PA/QA blends show, for the different functional groups analyzed, that the IR spectral band was not affected by the QA content (Fig. 10). Then, the calorimetric and spectroscopic measurements indicate that the PA/QN blends have specific interactions between the polymers, modifying the heat of fusion of the polyamides and the infrared spectra.

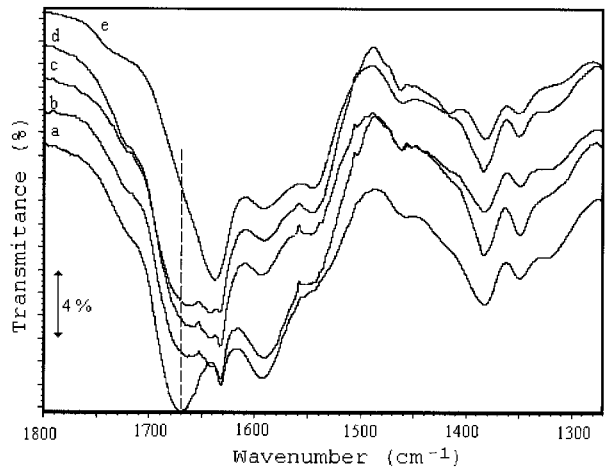

Figure 8 FTIR spectra for PA6/QN blends showing the displacement of the carbonyl band of the amide group of QN: (a) PA6; (b) PA6/QN 10/90; (c) PA6/QN 15/85; (d) PA6/QN 20/80; (e) PA6/QN 25/75.

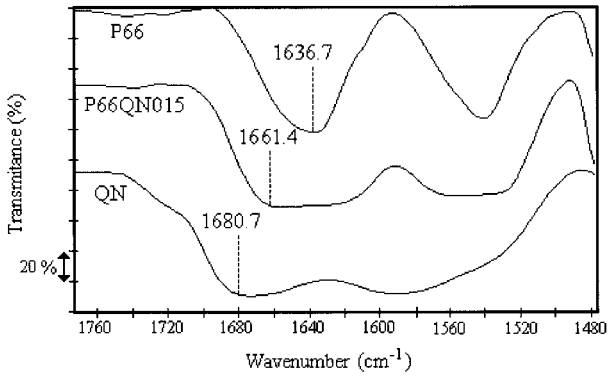

Figure 9 FTIR spectra for PA66/QN blends showing the shifting and widening of the carbonyl band.

Microscopy

The PA66/QA morphology observed by optical microscopy shows evident phase segregation in all the composition ranges (Fig. 11), revealing that there is no compatibility between PA66 and chitin. PA6/QA samples present spherulitic morphologies with the characteristic Maltese cross pattern (Fig. 12). The SEM images of these samples (Fig. 13) show a globular well-delimited

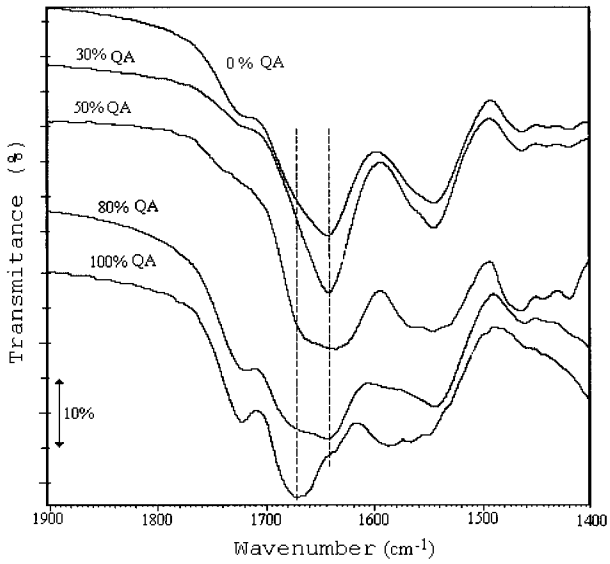

Figure 10 FTIR spectra for PA6/QA blends.

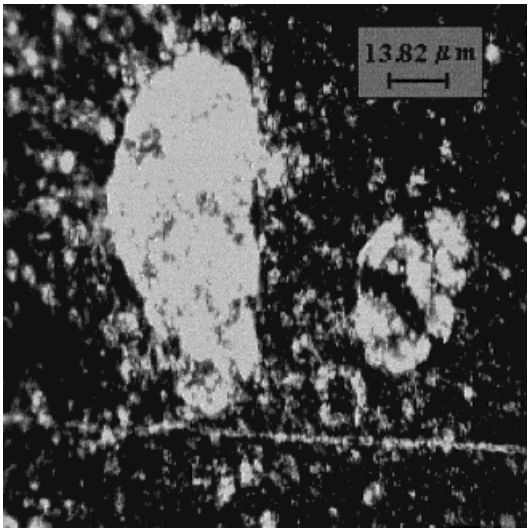

Figure 11 Cross-polarized optical micrograph of a PA66/QA 50/50 blend (500×).

amorphous phase (gray zones on Fig. 12). The morphology of the other phase is like a disk and it is most probably semicrystalline and responsible of the bright regions on Figure 12. This kind of morphology is more evident on blends with smaller QA content, such as in Figure 14. The observed conical shape, perceived also on QN/PA4 blends[21] and pure PA6,[22] is probably because the spherulitic growth of the upper region, outside the solution, is delayed. These results agree with the FTIR measurements, indicating an absence of

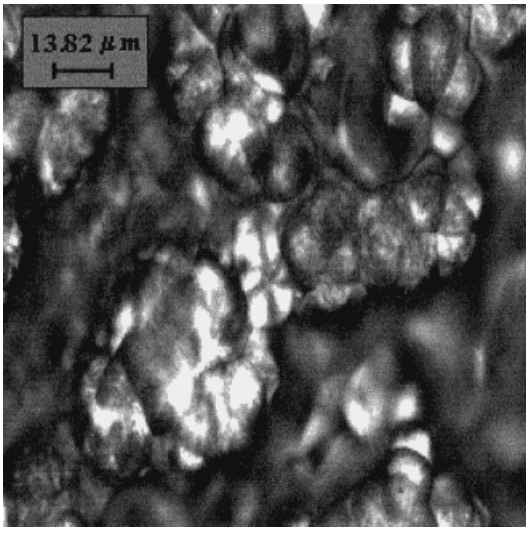

Figure 12 Cross-polarized optical micrograph of a PA6/QA 70/30 blend (500×).

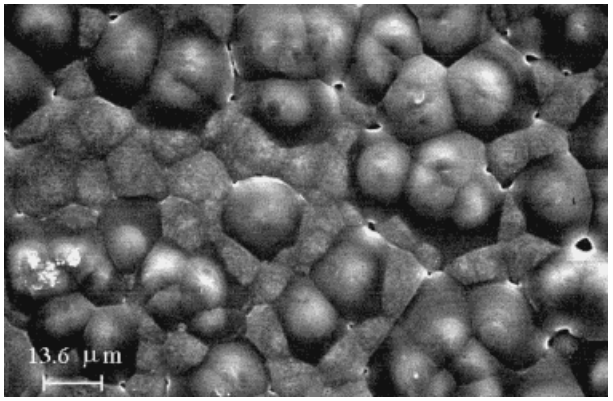

Figure 13 SEM micrograph of a PA6/QA 70/30 blend (730×).

specific interactions in both PA6/QA and PA66/QA blends.

For polyamide/chitosan blends, the morphology is very different from those encountered with chitin. Spherulitic morphologies were detected on PA6/QN blends in all the composition ranges (Figs. 15 and 16). X-ray spectroscopy performed on the samples shows that the spherulites were semicrystalline polyamide encapsulated in amorphous chitosan, embedded in a continuous phase of chitosan and amorphous polyamide.[18] For this kind of sample, Dufresne and coworkers[22] reported different morphologies, but in their work, the PA6/QN blends were etched either with *m*-cresol or with a buffer solution of chitinases. The idea of this procedure was to eliminate the PA6 or the chitosan from the blend, respectively. For PA66/QN, fibrillar structures were found, changing shape with the QN content (Figs. 17 and 18).

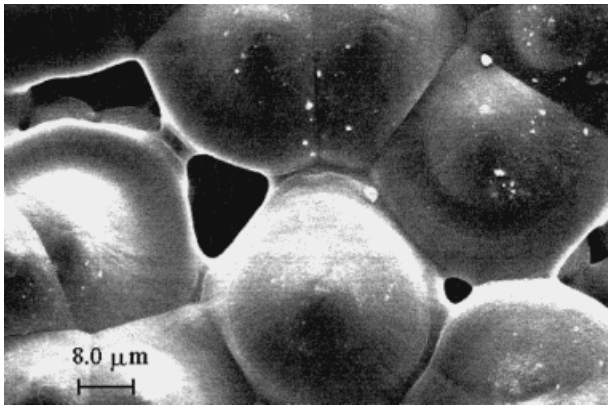

Figure 14 SEM micrograph of a PA6/QA 85/15 blend (1200×).

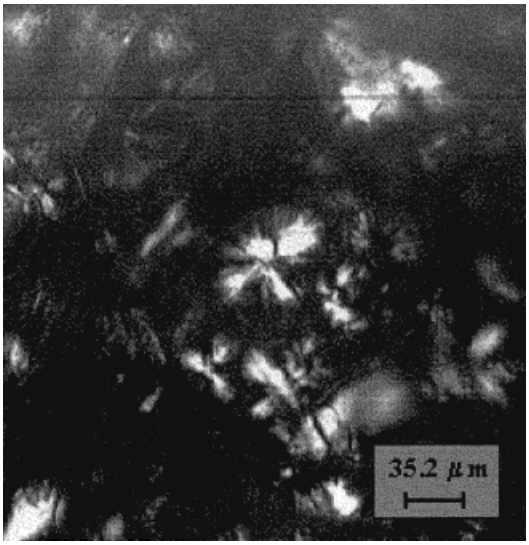

Figure 15 Cross-polarized optical micrograph of a PA6/QN 85/15 blend (200×).

The chemical composition of these structures has not been explained.

The morphological observations reinforce the FTIR and DSC measurements in the sense that PA/QN blends are more compatible, because of the stronger hydrogen bonds, compared to PA/QA blends. These measurements also show a qualitative difference in PA6/QN and PA66/QN interactions, but it is difficult to differentiate the compatibility degree.

In conclusion, for the four different blends, the following compatibilization sequence could be established:

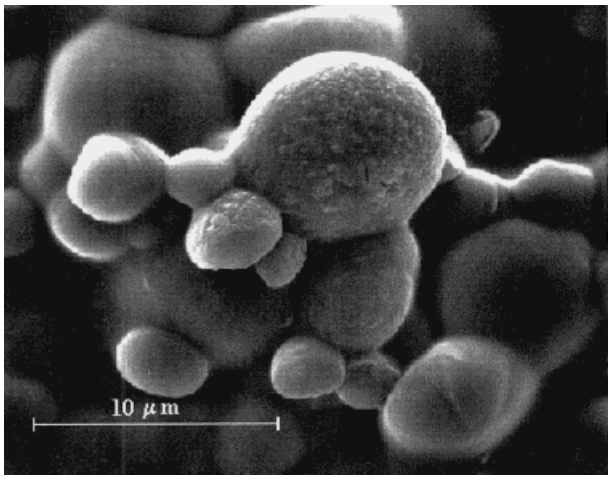

Figure 16 SEM micrograph of a PA6/QN 40/60 blend (3233×).

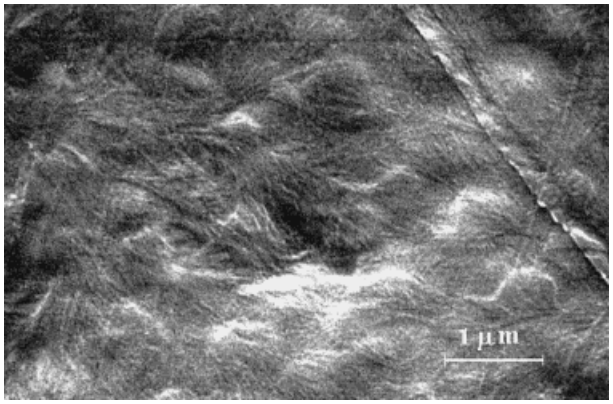

Figure 17 SEM micrograph of a PA66/QN 50/50 blend showing the spherical structures embedded in a fibrillar morphology.

$$\text{PA6/QN} \approx \text{PA66/QN} > \text{PA6/QA} > \text{PA66/QA}$$

It is interesting to note that the acetyl content on biopolymers influences the degree of compatibility; chitosan with 21% acetyl content is more compatible than is chitin with 51% acetyl content. This behavior could be explained, in addition to the steric impediment presented by acetyl groups on the formation of hydrogen bonds, assuming that at around 50% acetyl content the deacetylation process seems to alternate, giving to QA molecules a structural regularity and hindering polyamides to interact with them. However, this assumption must be validated with solid-state NMR studies (research in progress).

The better molecular packing properties of PA66 compared to PA6 (the latter has a melting point 45°C lower) promotes a dramatic change on the QA compatibility, while PA6 could be consid-

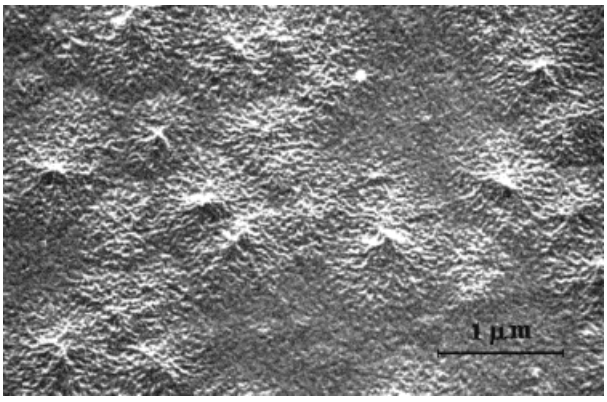

Figure 18 SEM micrograph of a PA66/QN 85/15 blend showing the fibrillar morphology.

ered QA-compatible, even if there are no appreciable hydrogen bonds, the PA66/QA blend is notoriously incompatible. The polyamide structural differences do not permit one to establish a compatibilization sequence with QN, but the morphological differences between PA66/QN and PA6/QN are evident, the former with fibrillar structures and the latter with encapsulated spherulites.

CONCLUSIONS

Using different analysis techniques, such as FTIR, DSC, and light and electronic microscopy, it is possible to differentiate, qualitatively, the degree of compatibility between PA6 and PA66 with chitin (49% deacetylated) and chitosan (79% deacetylated). The proposed compatibility sequence is PA6/QN $\approx$ PA66/QN $>$ PA6/QA $>$ PA66/QA. This result could be attributed to the better molecular packing properties of PA66 compared to PA6, the steric effect of chitin acetyl groups, and the possibility of an alternate deacetylation on the 49% deacetylated chitin.

The authors express their gratitude to the National Science and Technology Council (CONACyT) for its financial support.

REFERENCES

1. Viscoelasticity of Biomaterials; Glasser, W.; Hyoe, H., Ed.; American Chemical Society: Washington, DC, 1992.
2. Muzzarelli, R. A. A. Natural Chelating Polymers: Alginic Acid, Chitin and Chitosan; Pergamon: Oxford, 1973.
3. Flory, P. J. Principles of Polymer Chemistry; Cornell University: New York, 1953.
4. Boyd, R. H.; Phillips, P. J. The Science of Polymer Molecules; Cambridge University: New York, 1993.
5. Painter, P.; Park, Y.; Coleman, M. J Appl Polym Sci 1998, 70, 1273.
6. Albert, B.; Jerome, R.; Teyssie, P.; Baeyens-Volant, B. J Polym Sci Polym Chem 1986, 24, 551.
7. Silverstein, R. M.; Webster, F. X. Spectrometric Identification of Organic Compounds; Wiley: New York, 1998.
8. Weisskopf, K. Polymer 1985, 26, 1187.
9. Moore, G. K. Ph.D. Thesis, Trent Polytechnic, Nottingham, 1978, cited in Mazeau, K.; Chanzy, H.; Winter, W. T. Macromolecules 1994, 27, 7606.
10. Domszy, J. D.; Roberts, A. F. Makromol Chem 1985, 186, 1671.
11. Sawayanagi, Y.; Nambu, N.; Nagai, T. Chem Pharm Bull 1982, 30, 2413.
12. Muzzarelli, R. A. A. Chitin; University of Ancona: Italy, 1976.
13. Kurita, K.; Sannan, T.; Iwakura, Y. Makromol Chem 1977, 178, 2595.
14. Sannan, T.; Kurita, K.; Iwakura, Y. Makromol Chem 1975, 176, 1191.
15. Magill, J. H.; Girolamo, M.; Keller, A. Polymer 1981, 22, 43.
16. Inoue, M. J Polym Sci Polym Phys Ed A 1963, 1, 2697.
17. Rathke, T. D.; Hudson, S. M. Rev Macromol Chem Phys C 1994, 34, 375.
18. Guerrero, C.; González, V.; Romero, J. J Polym Eng 1997, 17, 197.
19. Guerrero, C.; González, V.; Ortiz, U. J Polym Eng 1999, 19, 109.
20. Kim, D. Y.; Ratto, J. A.; Blumstein, R. B. Polym Prepr 1991, 32, 112.
21. Ratto, J. A.; Chen, C. C.; Blumstein, R. B. J Appl Polym Sci 1996, 59, 1451.
22. Dufresne, A.; Cavaillé, J. Y.; Dupeyre, D.; García-Ramírez, M.; Romero, J. Polymer 1999, 40, 1657.